Chapter 5: Measurement results of microbolometer

In this chapter, several characteristics of microbolometers are evaluated including thermal impedance, TCR, resistance versus dissipated over power, and responsivity. Particularly, infrared optical measurement of the wavelength selectivity of resonant dielectric cavity microbolometer is made.

5.1 DC measurements for conventional microbolometer

DC measurement was performed to characterize the important characteristics of conventional micromachined microbolometer detectors such as that are shown in Fig.5.1. Microbolometers are isolated from the silicon substrate. The device (a) was fabricated in the method using surface micromachining that is explained in the conventional microbolometer. By DC measurement, the basic characteristics of a microbolometer can be revealed such as thermal impedance, TCR, resistance dissipated over power, and responsivity. The sheet resistance of the chromium bolometer layer was measured three days after deposition using a four-point-probe technique and found to be 330 ohm/square. Due to surface oxidation of chromium, the sheet resistance can change as much as 40 – 50 ohm/square after deposition.

Current-Voltage measurement (Hewlett-Packard, model HP4156B semiconductor parameter analyzer) was performed at atmospheric pressure and room temperature. Fifty second holding and long integration time was used to ensure thermal steady state measurement at each data point.

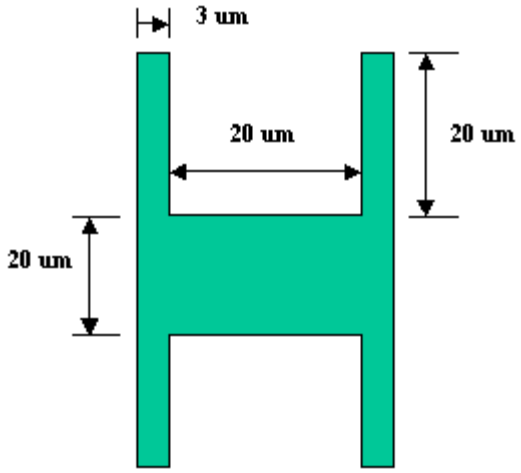

Figure 5.1 The dimensions of the conventional microbolometer fabricated using surface micromachining.

The results of the measurement are shown in Figure 5.2, which illustrates that an increasing the dissipated power in the bolometer decrease in resistance, which means the Temperature Coefficient of Resistance (TCR) is negative. As was shown in chapter 2, the bias current has to be increased without thermal run-away to maximize the responsivity. Therefore, the negative TCR is a desirable characteristic. The DC responsivity of the microbolometer can be found by taking the slope of the resistance – power plot as shown Fig.5.2. At this measured region, dR/dP is constant as 0.374 ± 0.008 ohm/μW by linear regression (regression coefficient is 0996). At 100 μA bias current, the DC responsivity is calculated to be 37.4 V/W. The linearity of the resistance over dissipated power can be found in

the measured temperature range from 298K to 304K. Equidistant curves indicate that dR/dP is constant over the measured temperature range (298-304K).

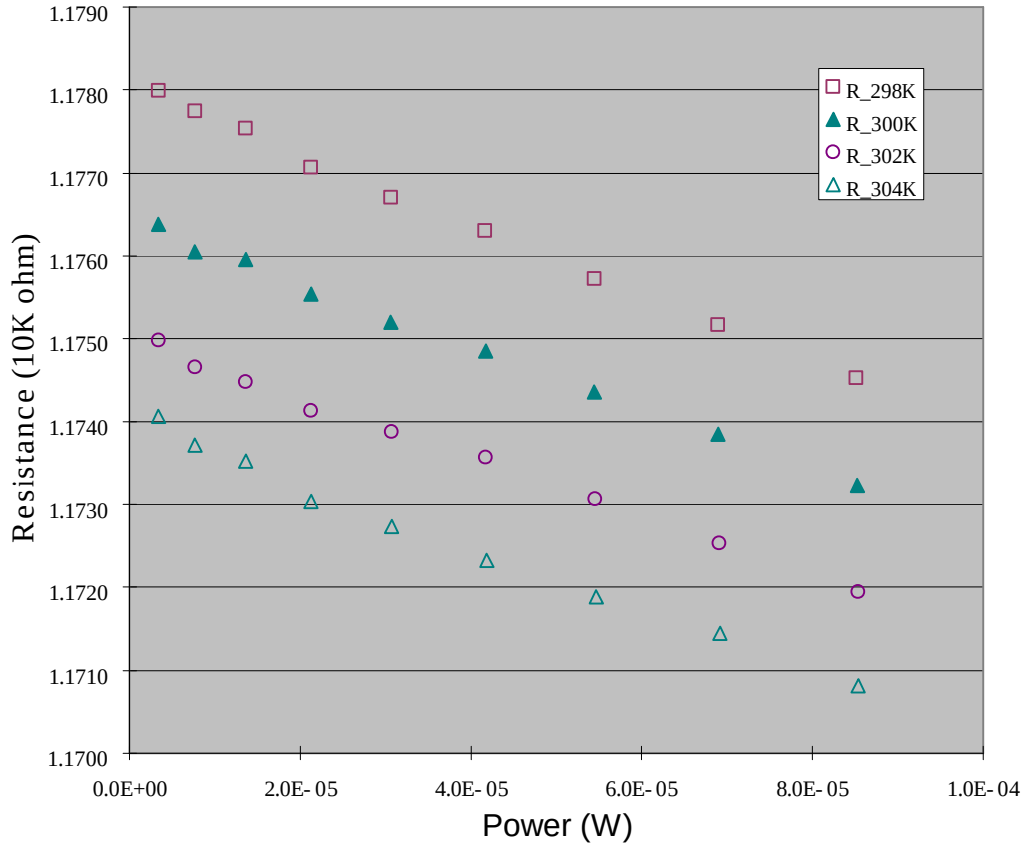

Fig 5.2 Resistance as a function of dissipated power for a conventional micromachined bolometer at various temperatures from 0.1 V to 1 V biased with step of 0.1V.

The TCR can be extracted by use of dR/dT and 1/R from the experimental data. As shown in Fig. 5.3, dR/dT, which are properties of material, is found to at

6.1 ± 0.075 ohm/K by linear regression (regression coefficient is 0.999). In the given measured temperature region, resistance over temperature is linear as well. Using the following relations, TCR can be found as

$$\alpha = \frac{1}{R} \cdot \frac{dR}{dT}. \tag{5.1}$$

Using the results shown in Fig.5.2, the TCR of deposited chrome is found from this data to be 0.0005 K^{-1} within the measured temperature range, in agreement with previous reports [1][2]. This value is lower than factor of five to ten compared with Tellurium, Bismuth and Vanadium Oxide.

The thermal impedance of the device can be found from knowledge of dR/dP and dR/dT:

$$\frac{dR}{dP} = \frac{dR}{dT} \cdot \frac{dT}{dP}. \tag{5.2}$$

Thermal impedance was found to be $6.13 \times 10^4 \pm 1.3 \times 10^3$ K/W. This value can be indirectly compared with previous reports. Eriksson reported that the thermal impedance of a leg-supported membrane microbolometer (6:10 ratio of leg width and length; 50μm x 50 μm membrane area) was 5×10^4 K/W and 4.4×10^6 K/W for atmospheric pressure and vacuum operation, respectively [3]. His research revealed that thermal impedance is constant if operational pressure range is lowered to less than approximately 0.01 mbar as well. After this pressure bound,

the thermal impedance is dominantly affected by the configuration of leg width-to- length ratio.

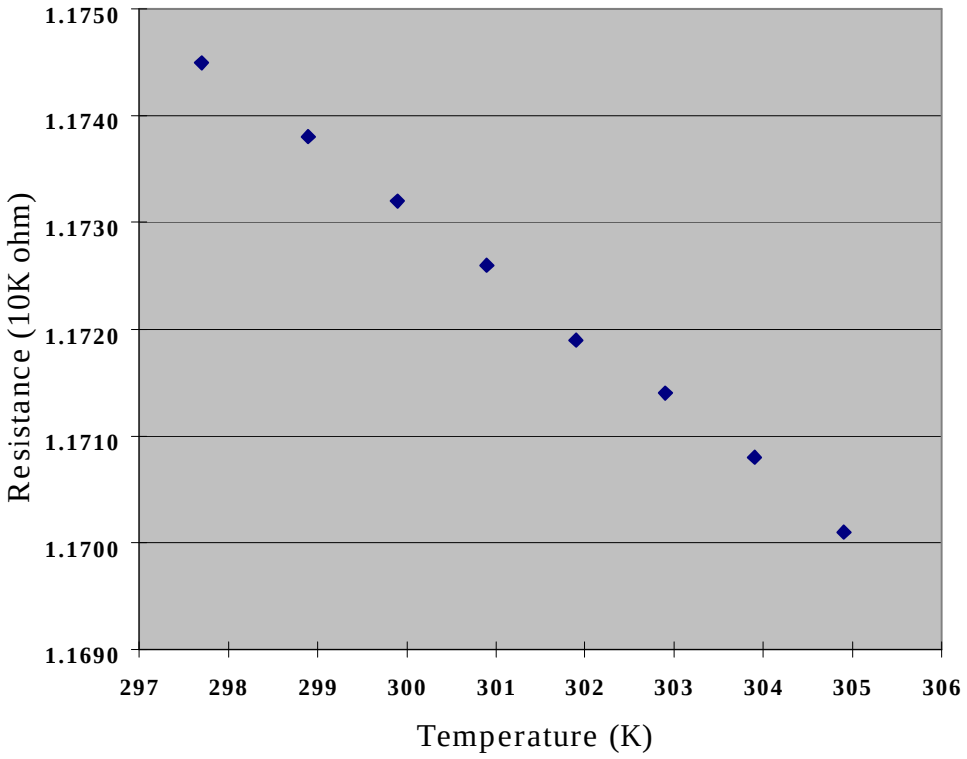

Figure 5.3 Resistance as a function of temperature for micromachined bolometer at 1 V bias.

Under the assumption of vacuum operation, the calculated thermal impedance of measured device should be 1.22 x 10^6 K/W, based on the calculation of DC thermal impedance. Therefore, the difference between measured and calculated thermal impedance suggests, also supported by previous publication [3], that the thermal impedance of the measured conventional

micromachined microbolometer is dominated by convection cooling at atmospheric pressure. Table 5.1 summarizes the result of the thermal impedance of conventional micromachined detector.

	Detector active size	The length of legs (μm)	The width of legs (μm)	Thickness of legs (μm)	Thermal impedance
(a)	50μm x 50μm	40	6	0.30	2.5×10^6 K/W
(b)	50μm x 50μm	60	2	0.50	5.5×10^6 K/W
(c)	26μm x 20μm	20	3	1.30	6.1×10^4 K/W

Table 5.1 The comparison of thermal impedance for membrane of different geometry. (a) and (b) are adopted from Erickson measured under vacuum [3]. (c) is measured data from the conventional microbolometer under ambient pressure by author.

5.2 Experimental setup

Under constant current biasing, the resonant dielectric cavity microbolometer was exposed to variable-wavelength infrared light (IR) to measure the spectral response. To ensure accurate IR response measurements, several factors were carefully measured and analyzed including wavelength, power, beam radius, and detector alignment.

5.2.1 Optical and electrical setup

Figure 5.4 illustrates the optical setup used to irradiate the microbolometer. Two different IR laser systems were used to determine the spectral response of the resonant cavity microbolometer.

A dual line (1.15 μm and 3.39 μm) helium-neon laser (Research Electro-Optics Inc.) and tunable infrared ultrafast laser system [9] were used in this study. The helium-neon laser emitted the monochromatic radiation specified by the manufacture. The ultrafast laser, however, has a broad spectral response that could be tuned from 2.4 to 15 um. Peak values from 2.75 to 4.5 um were used due to low power output outside that wavelength range. The broad spectral characteristics of ultrafast laser complicates the measurement of detector spectral response. For characterization of the microbolometer response, a single monochromatic wavelength laser source is better than broad band thermal or broadband laser source in order to easily control the incident laser power and to accurately measure the beam radius at the microbolometer for narrow band analysis. Therefore, if it is possible, a narrow banded monochromatic source can be more useful for making accurate measurement and analysis of detector responsivity.

The near-infrared line was used with an infrared viewer to align the beam collinear to a second visible helium-neon laser that emitted light at 0.632 μm.

---

[9] Tunable infrared ultra fast laser system manufactured by Coherent Inc. consists of Innova 200 argon ion pump laser, Mira model 900-B titanium: sapphire femtosecond laser, RegA model 9000 titanium: sapphire regenerative amplifier, OPA model 9800 optical parametric amplifier, and DFG difference frequency generator. Chromex Inc. model 500 IS/SM spectrometer was used to characterize the spectral output of system.

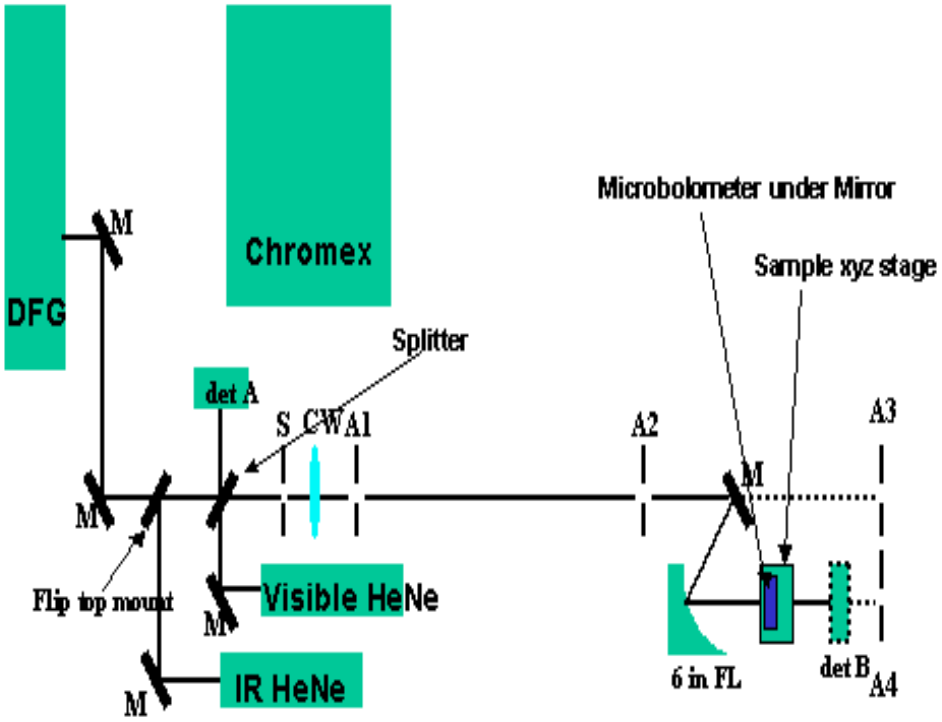

Figure 5.4: Optical setup used to irradiate the microbolometer. The visible and infrared helium-neon lasers are made collinear to allow alignment of the beam on the microbolometer active area. Detector position is controlled with a three-axis stage. M: Mirrors, BS: beam splitter, Det A and Det B: power meters, A1-4: iris apertures, S: Shutter, DFG: difference frequency generator.

Use of the near infrared line was necessary because the wavelength sensitivity range of the infrared viewer was limited to 1.5 μm. The visible and infrared helium-neon lasers were made collinear to allow alignment of the beam on the microbolometer active area. The visible helium-neon laser was used to

center the laser beam on the microbolometer infrared active area while the microbolometer was imaged through a surgical microscope, which has more depth of focus than a conventional microscope. Use of the visible laser was essential because of the small size of the microbolometer active area and the limited magnification of the infrared viewer. Far more precise alignment was achieved by use of the surgical microscope than could be accomplished with the infrared viewer alone. Figure 5.5 shows the setup of microbolometer and probes. The beam-turning mirror is located above microbolometer. This beam mirror directs the beam vertically down onto the device. Once alignment established on the microbolometer active area, the visible and near infrared lines were blocked.

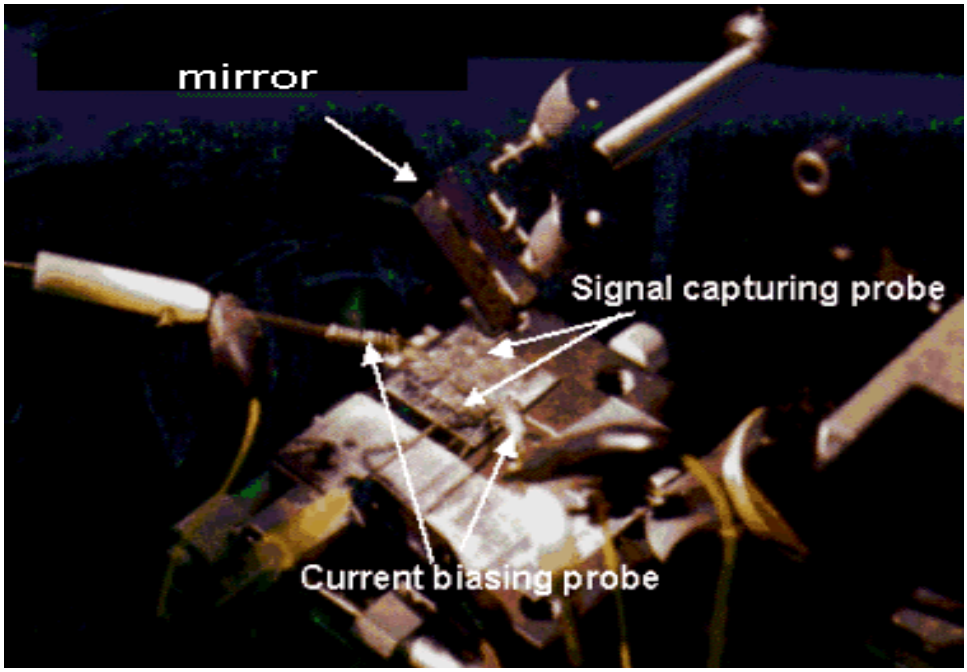

Figure 5.5 The probes and beam-turning mirror setup on the XYZ stage.

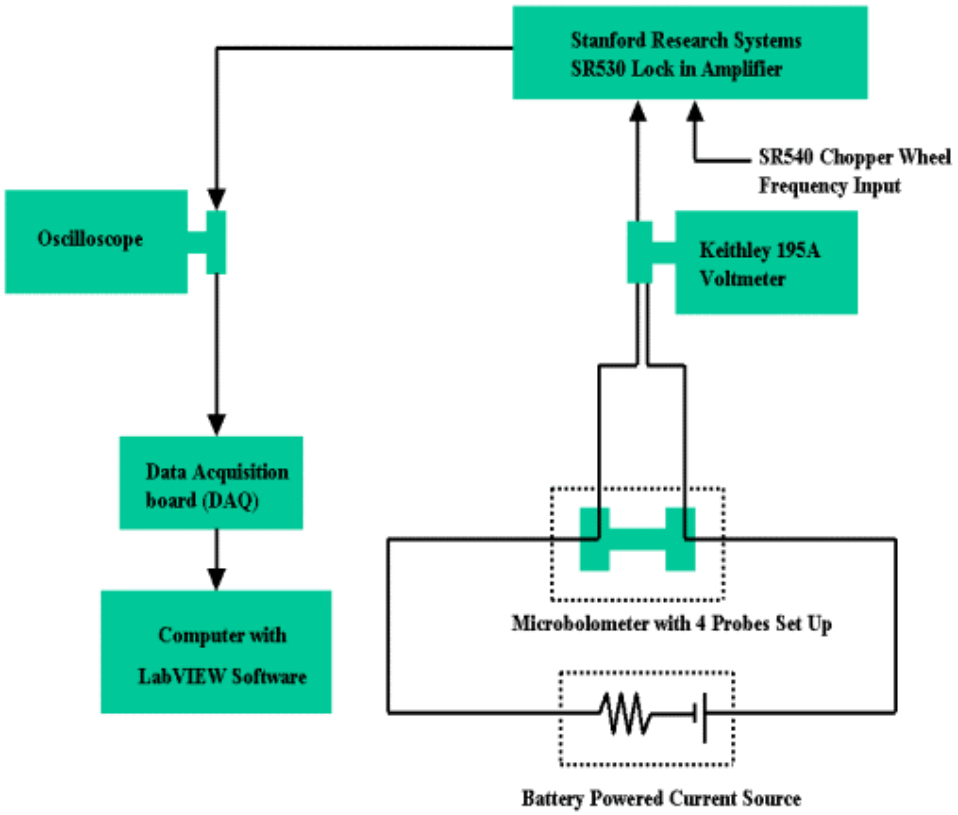

Figure 5.6 Schematic of the circuit and instrumentation used to make an incoming infrared responsivity measurement: voltmeter (Keithley model 195A) for confirming the bias condition, and oscilloscope for finding the best alignment between the incident beams and detector active area.

5.2.2 Power and spot size measurement

Determination of the spot size of the IR laser beam is fundamental to the accurate measurement of the microbolometer response. Accurate measurement of spot size and incident IR power allowed comparison of the response for different wavelength response.

The incident IR power was measured during measurement of microbolometer output voltage. The power from incoming infrared laser was measured at the point A for the each wavelength. As shown in Fig.5.3, a CaF_2 beam splitter divided the light between the path in which the microbolometer was placed and a power detector A (Molectron Inc. EPM2000 power meter and PM-3 head). With the microbolometer removed but all other optics in place and the beam aligned straight and level between apertures A1 and A2 (see Fig. 5.3), the power at detector B (det B) was measured. The ratio of power at detector A to detector B was then used to correct the power recorded with detector A during the experiments.

To measure the spot size with beam radius, a scanning knife-edge method was adopted, which is simple and widely used for spot size measurements [4]. In this method, one scans knife transversely across the beam profile while detecting the transmitted power on a large area photo-detector. By choice of the appropriate “clip width”, the plot of transmitted power as a function of knife position allows for a measure of the beam radius, the resolution and accuracy which is limited only by the stage upon which the knife is fixed.

If the position on the optical axis (e.g. position of microbolometer) of interest is known precisely, only a single scan is necessary to characterize the beam radius. For example, if the minimum spot size is needed, several scans across the optical axis can be made.

Software[10] (in LabVIEW, vers 5.1) was developed to measure the spot size of the laser beam with the knife-edge technique using a computer controlled stage and energy meter [5]. The software uses instrument drivers for the SD Instruments Inc. micromanipulator, which holds the knife, and Molectron Inc. dual energy and power meter. The micromanipulator is a 4-axis positioner that is commanded via a RS-232 serial line, and the energy meter is controlled with the general purpose interface bus (GPIP).

The radius of the focused beam was measured at several points along the optical axis with an automated knife-edge technique (ISO, 1999). In order to make an accurate measurement of the responsivity, it was important to make the incident beam size larger than the microbolometer infrared active area. Thus, a beam radius of 200 – 250 μm was used. In order to keep the optical setup somewhat compact, instead of using a focusing lens with a long focal length (and hence a larger spot size), the microbolometer was positioned in front of the focus at the position of the targeted beam radius. Accurate spot size measurement was done before and after all of the IR measurement. As long as the optical apparatus remained intact, a single measurement of spot size was sufficient for many response measurements.

[10] Program written by Dan Hammer.

5.3 Measurement results

5.3.1 Modulation frequency response

Using the setup described in the previous section, characterization of the microbolometer response to IR irradiation was performed. Prior to the measurements, it was first necessary to determine the appropriate modulation frequency for the operation of the microbolometer. The output voltage can be found as

$$V(l) = I_b \cdot \frac{dR}{dT} \cdot \Delta T = I_b \cdot \frac{dR}{dT} \cdot P_{absorbed}(l) \cdot Z_{thermal} \cdot \frac{1}{\sqrt{1+w^2 t^2}}. \qquad (5.2)$$

where the variables are defined in Eqn.(2.4) in chapter 2.

The incoming infrared can be affected by the chopper-modulated frequency as shown Eqn. (5.2). Figure 5.6 illustrates the measured voltage output of the microbolometer in response to IR irradiation by modulating the incoming frequency. The lock-in was used to detect small AC signals from the microbolometer caused by infrared excitation. A lock-in amplifier can make accurate measurements of small signals even when the signals are obscured by broadband noise sources, which may be larger than the signal. Essentially, a lock-in is a filter with narrow bandwidth that is tuned to the frequency of the signal set by the chopper. Such a filter will reject most unwanted noise to allow the synchronizing signal to be measured.

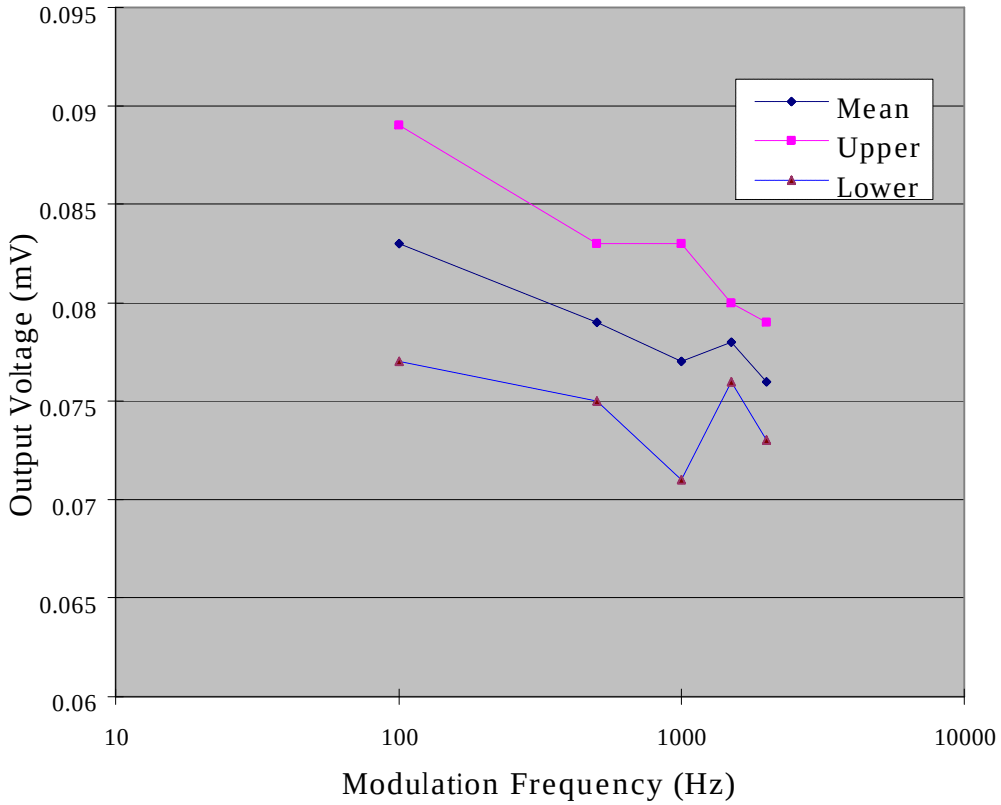

Figure5.7 Measured output voltage of resonant dielectric cavity microbolometer without gold mirror as a function of modulation frequency in response to the HeNe infrared laser at 3.39 μm. Detector specification: active area 26 μm x 20 μm; 20 μm leg length; 3 μm leg width; 230 ohm/square chromium bolometer layer sheet resistance; no gold mirror coating on the backside of microbolometer. Lock in amplifier settings: sensitivity 10 mV, time constants pre = 1 msec, post = 0.1 msec.

As long as the same experimental conditions at the device are unchanged, the thermal impedance, absorbed power, bias current, and TCR can be considered constants in their contribution to detector output voltage. Thus, the only variable that causes the output voltage to change is chopper modulation frequency. Due to this frequency dependency, at the high frequency, the voltage output rolls off at a single wavelength measurement. In addition, frequency-related noise voltage could be reduced at the high frequency if 1/f noise is dominant. Therefore, it is desirable to select a higher chopper modulation frequency that is lower than the frequency where the voltage output rolls off. As shown in Fig.5.6, independent voltage output for modulated frequency is obtained within the measured modulated frequency. This result can be supported by calculation of thermal time constant. The thermal time constant was found to be as 0.1 m second based on the calculated thermal impedance and heat capacity[11]. However, due to convection cooling, the actual thermal time constant can be faster and it was found to 2 μ second. From the results, if $\omega^2\tau^2$ is much less than 1 ($\omega^2\tau^2 << 1$), modulated frequency dependent term of output voltage can be abbreviated as 1. Base on relationship of $\tau = 1/(2\pi f_{3dB})$, the 3 dB roll off frequency of output voltage can be found approximately at 8×10^4 Hz. The purpose of this measurement is to find the appropriate chopping frequency that did not affect measurement of the response and minimize the possible noise voltage. The modulated frequency chosen in this experiment was 1500 Hz.

[11] Heat capacity = 4.23×10^{-11} J/K , DC thermal impedance = 2.39×10^6 K/W.

5.3.2 Irradiance, output voltage, and responsivity measurement

Several optical measurements were performed on the resonant dielectric cavity microbolometer. Active area of device, the length of leg, the width of legs, and the thickness of membrane are 20 μm x 26 μm, 40 μm, 5 μm, and 0.96um, respectively. The sheet resistance of chromium is 230 ohm/sqr. The 200 Å gold layer was deposited as mirror on the back of microbolometer. The current of 100 μA was applied for biasing the device. For the basic characterization of the device, the resistance versus power dissipation, the resistance over temperature, and thermal impedance were measured as 0.204 ± 0.003 ohm /μW (value of linear regression, Regression coefficient = 0.991), 4.84 ± 0.06 ohm/K, and 4.21 x 10^4 ± 6.19 x 10^2 W/K, respectively.

Unlike the conventional microbolometer, the resonant dielectric cavity device has the gold mirror layer that can affect the thermal impedance of device. To see the difference of gold mirror layer on thermal performance, the dc thermal impedance of resonant dielectric device with and without gold layer were calculated as 0.43 x 10^6 W/K and 2.39 x 10^6 W/K, respectively, based on the calculation of DC thermal impedance. These values are much larger than the measured thermal impedance. Due to the operation at ambient pressure, the thermal impedance is dominant by thermal loss to air. Therefore, the effect of gold mirror is reasonably ignored for the estimation of thermal impedance.

For the 1.15 and 3.39 μm lines of the monochromatic HeNe laser, responsivity can be calculated based on measured voltage output and incident flux.

The responsivity is

$$\Re(\lambda) = \frac{V(\lambda)}{f_{incident}(\lambda)} = \frac{V}{E(\lambda) \cdot A_d} \quad \text{[V/W]}, \tag{5.3}$$

and

$$\Re(\lambda) = \frac{V(\lambda)}{f_{incident}(\lambda)} = I_b \cdot \frac{dR}{dT}\frac{dT}{dP} \cdot \frac{P_{absorbed}(\lambda)}{f_{incident}(\lambda)} = I_b \cdot Z_{thermal} \cdot \frac{dR}{dT}\frac{1}{\sqrt{1+\omega^2\tau^2}} \cdot h(\lambda), \tag{5.4}$$

where the terms are defined in chapter 2.

$P_{incident}$ is defined as the power measured at point B as shown in Figure 5.3. To determine the incident flux ($f_{incident}$), the incident power ($P_{incident}$), the beam radius of the incoming infrared, and the size of detector have to be measured. Figure 5.8 shows the output voltage in response to the incident power at a wavelength of 3.39 μm. The measured signal output with the infrared blocked is the noise voltage under bias. After the incoming infrared beam is unblocked, the voltage response at the specified wavelength was measured. Figure 5.9 gives the irradiance on the microblometer at the wavelengths of 1.15 and 3.39 μm. Irradiance is determined by the size and power of incoming infrared beam.

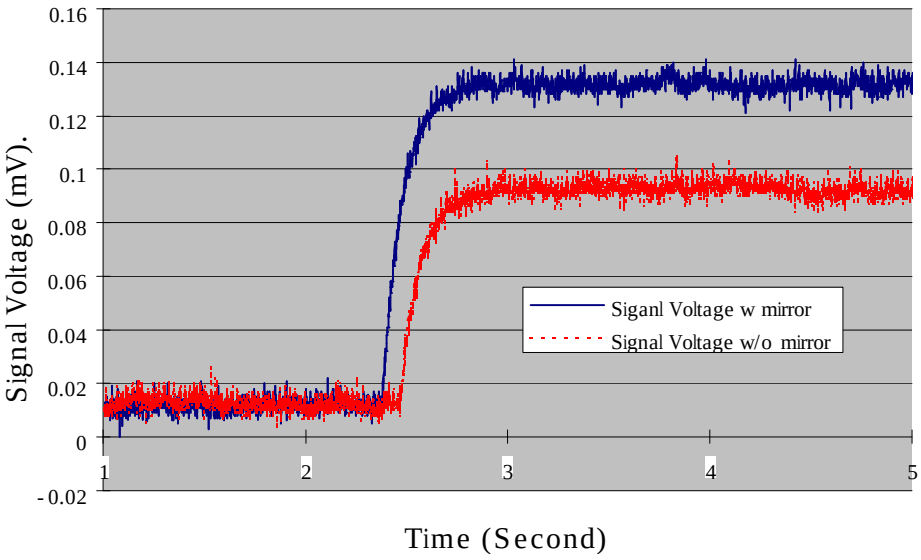

(a)

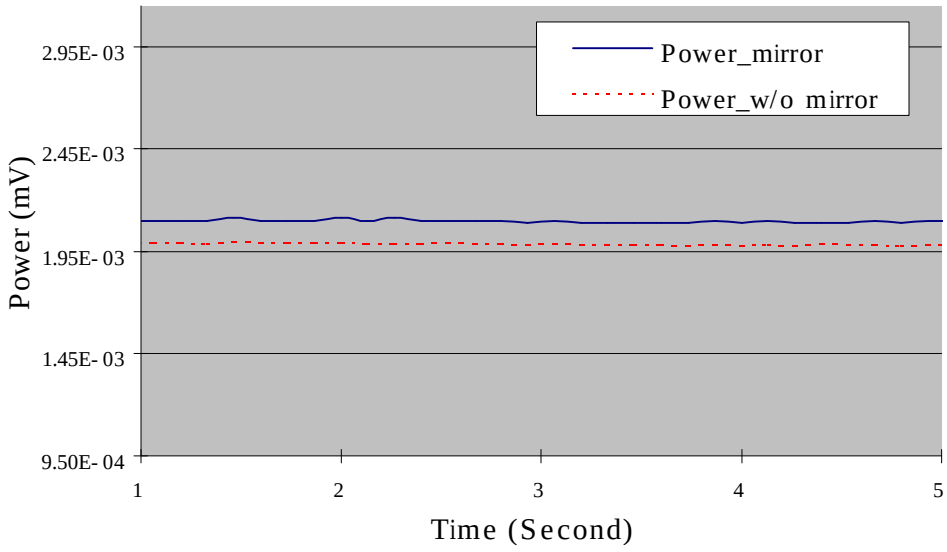

(b)

Figure 5.8 Measured signal voltage (a) of resonant dielectric cavity with gold mirror and without gold mirror biased at 100 μA in response to IR power (b) at 3.39 μm. The chopping frequency is 1500 Hz.

Irradiance is

$$Irradiance(l) = \frac{P_{incident}}{p \cdot r(l)^2}, \tag{5.5}$$

where r is the radius of incident infrared beam.

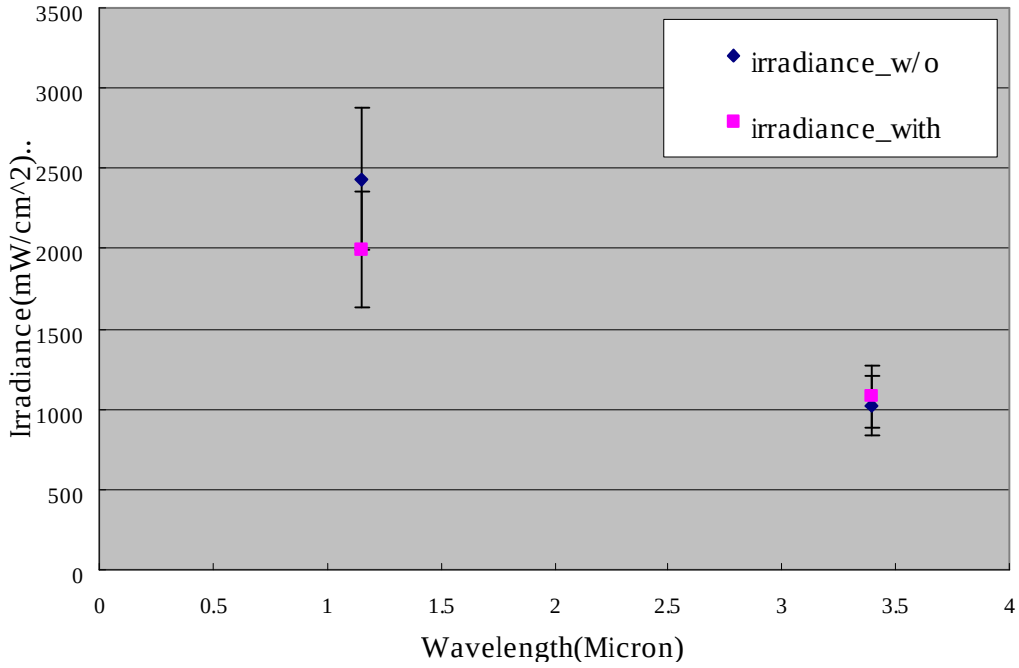

Figure 5.9 Irradiance of incident infrared at 1.15 and 3.39 μm. irradiance_w/o and irradiance_with are the irradiance of resonant dielectric cavity microbolometer with having gold mirror and without having gold mirror, respectively.

For this irradiance calculation, the radius of beam at 1.15 and 3.39 μm is measured as 200 ± 20 and 250 ± 20 μm, respectively. Power at the point B (see Fig. 5.3) on devices with mirror and without mirror is 3.15 and 2.58 mW at the 1.15 μm. At the time of measuring the spectral response at 3.39 μm, the power on devices without mirror and without mirror is 1.99 and 2.09 mW, respectively. In this plot, the different incident power level causes the difference of irradiance at the same wavelength for the experiments with and without mirror.

If the active area of the microbolometer is larger than the size of the incident infrared beam, the power density (flux) on the active area of the microbolometer equals the measured irradiance. However, if the active area of the detector is smaller than the spot size, the incident flux on the microbolometer is found from,

$$f_{incident}(l) = Irradiance(l) \cdot A_{dec}, \tag{5.6}$$

where A_{dec} is the detector active size.

From the measured voltage, incident power, and known information such as thermal impedance, bias current, and the resistance change versus temperature, the power coupling efficiency can be calculated as

$$h = \frac{V}{f_{incident}} \cdot \frac{1}{I_b \cdot Z_{thermal} \cdot \frac{dR}{dT}} = \frac{P_{absorbed}}{f_{incident}}. \tag{5.7}$$

Figure 5.10 and 5.11 illustrate the results of measurement and simulation for power coupling efficiency, output voltage, and responsivity. The subscript of with and without is for the experimental and simulated results of the resonant dielectric cavity microbolometer with gold mirror and without gold mirror. Strictly speaking, the device absent of the gold mirror layer should not be called as a resonance device. The annotation is used merely to distinguish the two configurations. The results indicate that the measured and calculated power coupling efficiency, output voltage, and responsivity agree to within 20%. Table 5.2 summarizes the result of the microbolometer for incoming infrared wavelengths of 1.15 and 3.39 μm.

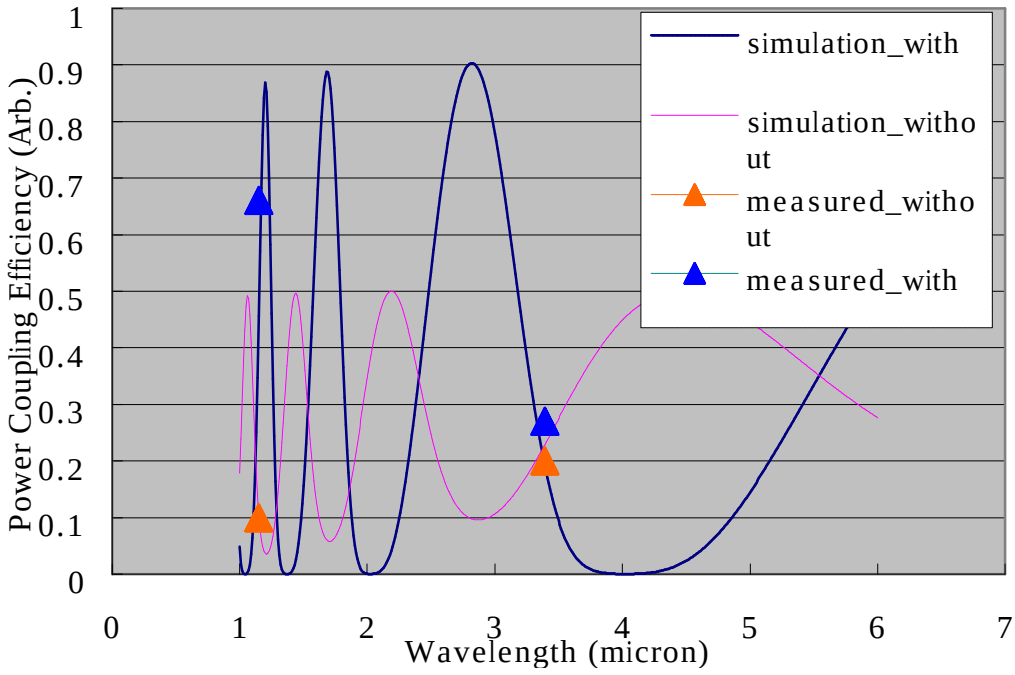

Figure 5.10 Comparison of power coupling efficiency between simulated and measured data.

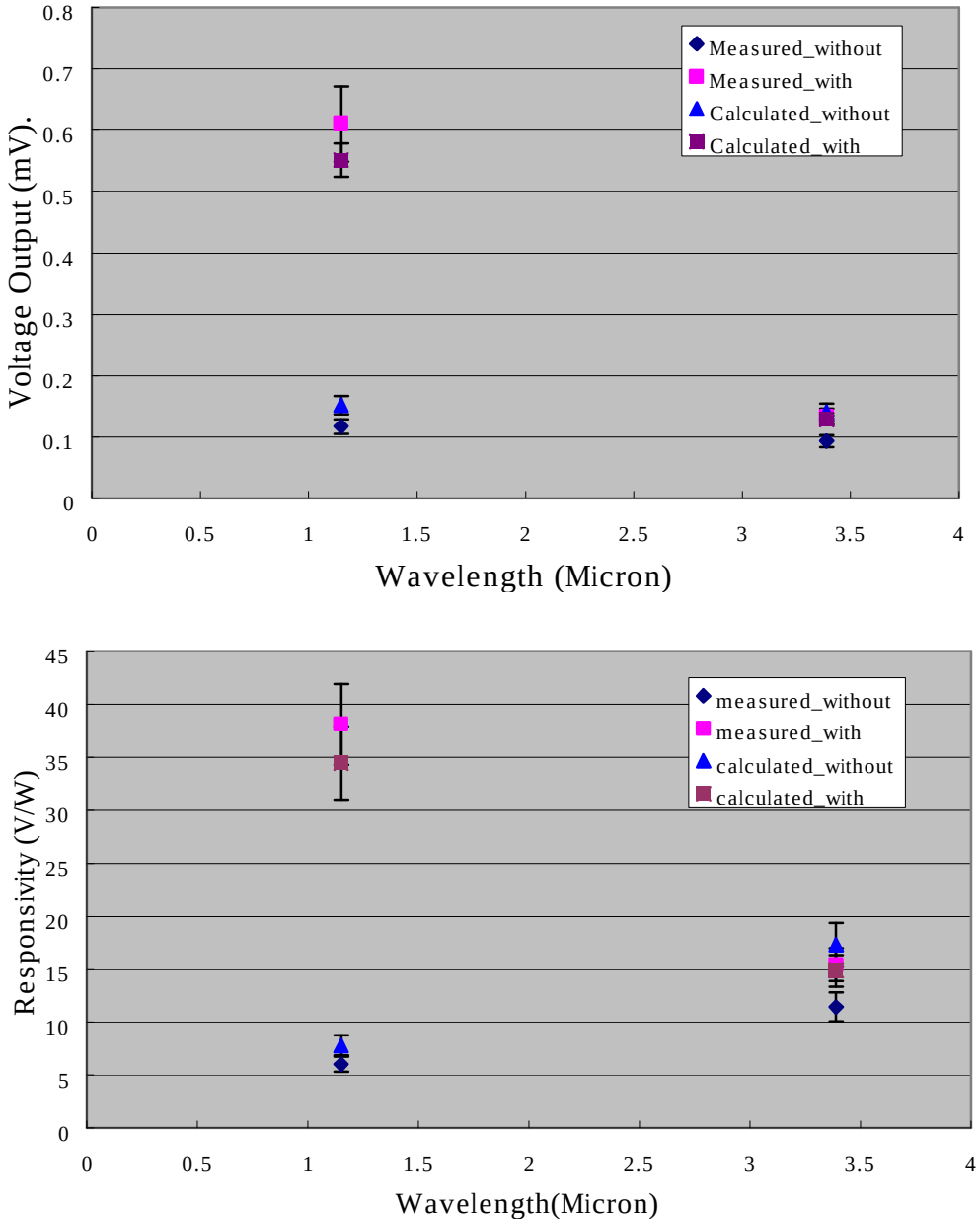

Figure 5.11 The measured and calculated results of output voltage and responsivity of the microbolometer biased at 100 μA in response to1.15 and 3.39 μm light.

	1.15 μm		3.39 μm	
	W/o mirror	Mirror	W/o mirror	Mirror
Output Voltage (mV)	0.117 ± 0.004	0.610 ± 0.004	0.093 ± 0.002	0.133 ± 0.002
Incident Power at point B (mW)	3.15 ± 1.422×10^{-2}	2.58 ± 3.019×10^{-2}	1.99 ± 4.26×10^{-3}	2.09 ± 6.26×10^{-3}
Spot size of beam (μm)	200 ± 20	200 ± 20	250 ± 20	250 ± 20
Irradiance (mW/cm^2)	2434.38± 407.97	1996.19± 431.97	1022.69 ± 183.59	1077.19 ± 192.59
Device Active Area (cm^2)	8×10^{-6} (20μm x 40μm)	8×10^{-6} (20μm x 40μm)	8×10^{-6} (20μm x 40μm)	8×10^{-6} (20μm x 40μm)
Incident flux on active area (mW)	0.0194 ± 0.00326	0.0160 ± 0.00345	0.00813 ± 0.00147	0.00861 ± 0.00154
Power Coupling efficiency	0.10 (measured)	0.66 (measured)	0.20 (measured)	0.27 (measured)
Responsivity (V/W)	5.99 ± 1.3	38.17 ± 7.0	11.32 ± 2.2	15.38 ± 2.8

Table 5.2 Summary of the results of microbolometer characterization using the HeNe infrared laser at 1.15 and 3.39 μm.

The characterization of the microbolometer at wavelengths of 1.15 and 3.39 μm illustrates that the coupling efficiency is wavelength dependent. However, information from two wavelengths is insufficient for model verification. The clearest method of verification of the power coupling model would be by measurement of the infrared response at other narrow wavelengths besides 1.15 and 3.39 μm. By measuring narrow band response, the entire spectral response could be recontructed. Due to limited availability, only four more different wavelengths produced by the ultrafast laser system were used to verify the model. Unlike the monochromatic characteristic of the HeNe Laser, the ultrafast laser exhibited the fairly broadband behavior as shown in figure 5.11.

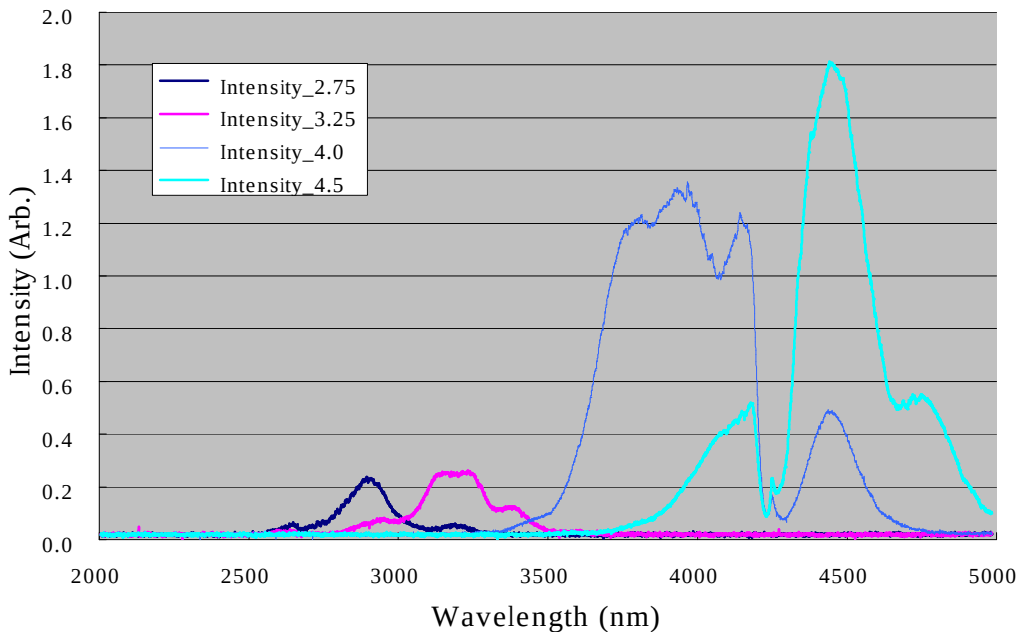

Figure 5.12 Spectrum of output from ultrafast laser system at the wavelengths used in the experiments. (characterized and measured by Dan Hammer)

It is shown that there is the strong absorption of 4.30 μm wavelength by CO_2 in the atmosphere. Due to the broad spectral characteristic of the ultrafast laser, Eqn. (5.2), the expression of voltage output must be changed into generalized as

$$V = I_b \cdot \frac{dR}{dT} \cdot Z_{thermal} \cdot \frac{1}{\sqrt{1+w^2 t^2}} \int_{l_1}^{l_2} P_{incident}(l) h(l) dl, \tag{5.8}$$

where λ_1 and λ_2 are the start and end of spectral bandwidth, respectively.

Incident power is distributed in the region of radius of beam. The measured radius of peak of wavelength is the averaged radius of incoming wavelengths consisting the broad bandwidth. This averaging effect of radius in the spectral range of specified peak wavelength may causes the difference between measured and calculated of voltage output. Using the spectral shape of Figure 5.12, the absorbed power on detector can be found as

$$P_{absorbed} = \int dx \int dy \int dl \cdot h(l) \cdot S(l, x, y), \tag{5.9}$$

where $S(l, x, y)$ is the unit of $\frac{Watts}{cm^2}\frac{1}{cm}$. $S(l, x, y)$ consists of power in area of *dxdy* and power in wavelength range of δλ.

The reason of averaged irradiance is used is it is not possible to measure the beam radius of each monochromatic component of the incident broadband

laser light produced by ultrafast laser. For example, the measured spot size at the peak value of 2.75 μm is the averaged valued of spot size from 2.5 μm to 3.3 μm. The spot size should be measured at each wavelength to accurately determine irradiance. In the calculation, irradiance is inversely proportional to the square of the beam radius. The unknown of spot size of incoming infrared may be factor to cause the ambiguity. The peak wavelength in Fig.5.13 represents the peak value of the incoming light.

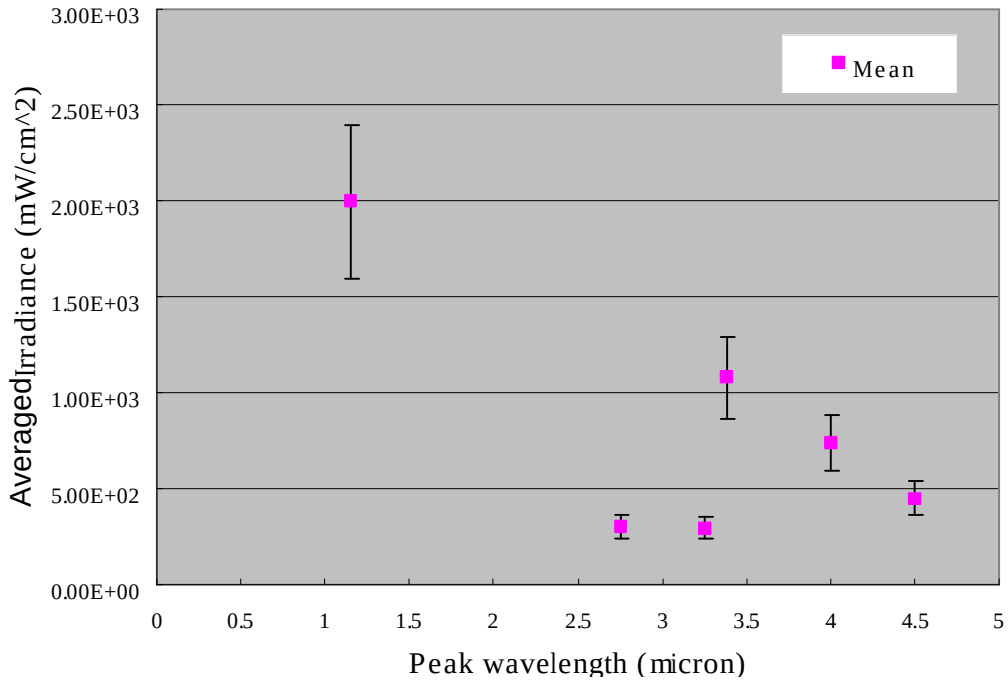

Figure 5.13 Averaged irradiance incident on the resonant dielectric cavity microbolometer from HeNe (1.15 and 3.39 μm) and ultrafast (2.75, 3.25, 4 and 4.5 μm) laser.

Figure 5.13 illustrates the comparison of output voltage between measured data and calculated data. Using the Eqn. (5.8), output voltage is calculated in the bandwidth of incoming infrared. As shown previously, for the 1.15 and 3.39 μm wavelengths, the prediction of voltage can be made within 20% error range. The simulation and measurement for the broadband wavelengths followed similar trends despite the fact there was a ambiguity due to lack of information about beam radius of each monochromatic component of the incident broadband laser light produced by ultrafast laser. Even though the voltage output of peak value of 2.75 μm is similar to 3.25 μm, responsivity of 2.75 μm was much larger than 3.25 μm. This means that more coupling is generated for less incident power.

Figure 5.15 presents the responsivity of resonant dielectric cavity microbolometer at all measured wavelengths. The results clearly indicate that the device with gold mirror has large responsivity at the resonant point than the device without gold mirror. However, the results do not completely confirm the model.

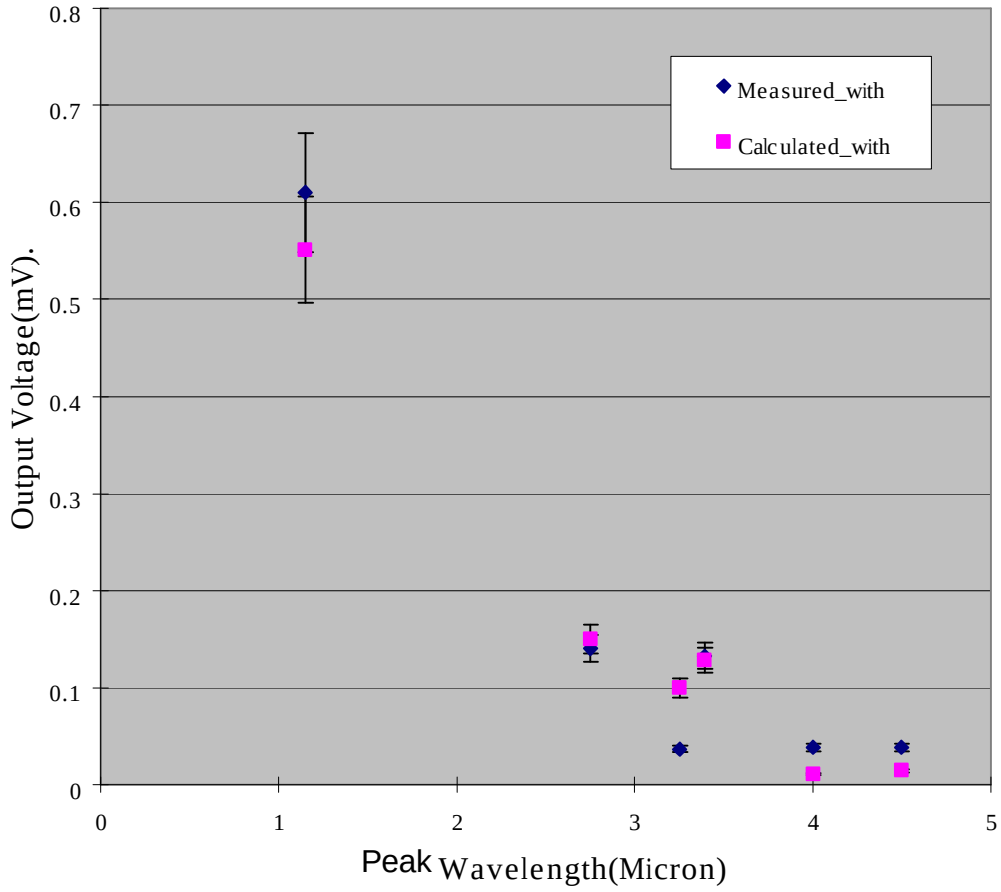

Figure 5.14 Output voltage of resonant dielectric cavity microbolometer in response to 1.15 and 3.39 μm monochromatic light and 2.75, 3.25, 4, and 4.5 μm broadband light.

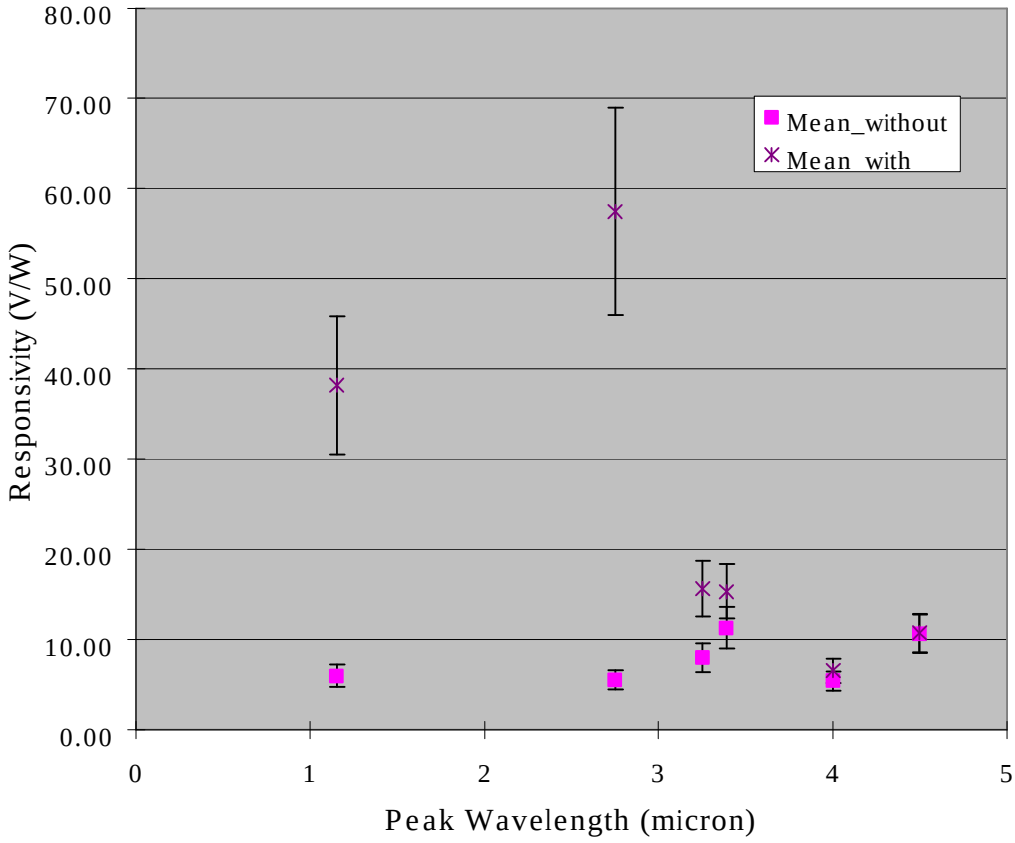

Figure 5.15 The responsivity of the resonant dielectric cavity microbolometer with gold mirror and without gold mirror.

5.4 Noise measurements

Noise measurements were made with a Stanford Research SR 530 lock-in amplifier while the microbolometer is biased at 100 μA as shown in Fig.5.4. The lock in measured the noise across the microbolometer over a 10% bandwidth of the selected frequency. Figure 5.15 shows the voltage noise as a function of frequency at room temperature. The decreasing noise with frequency suggests that 1/f noise is dominant for this device. If the responsivity is known as a function of frequency at the bias current, the noise equivalent power (NEP) can be calculated by dividing the voltage noise by the responsivity:

$$NEP[W/\sqrt{Hz}] = \frac{V_n/\sqrt{Hz}}{\Re_{dc}}. \qquad (5.10)$$

From 100 Hz to 2000 Hz, the responsivity is not affected by the modulated chopping frequency, namely, does not roll off. NEP is the minimum power from the incoming infrared beam needed to distinguish the signal voltage from the noise voltage. For the resonant dielectric cavity enhanced microbolometer, the dc NEP at the modulation frequency of 1500 Hz can be calculated as 5 x 10^{-8} W/$(Hz)^{-1/2}$. (Noise voltage 1x 10^{-6} V/$(Hz)^{1/2}$, dc responsivity is 21.6 V/W and biased at 100 μA). For the different incoming wavelength, the system NEP can be different because of responsivity associated with power coupling efficiency. From the result of NEP, The detectivity (*D**) at the 1500 Hz modulation frequency can be calculated as 6.9 x 10^4 cm $(Hz)^{1/2}$/W by using Eqn.2.9.

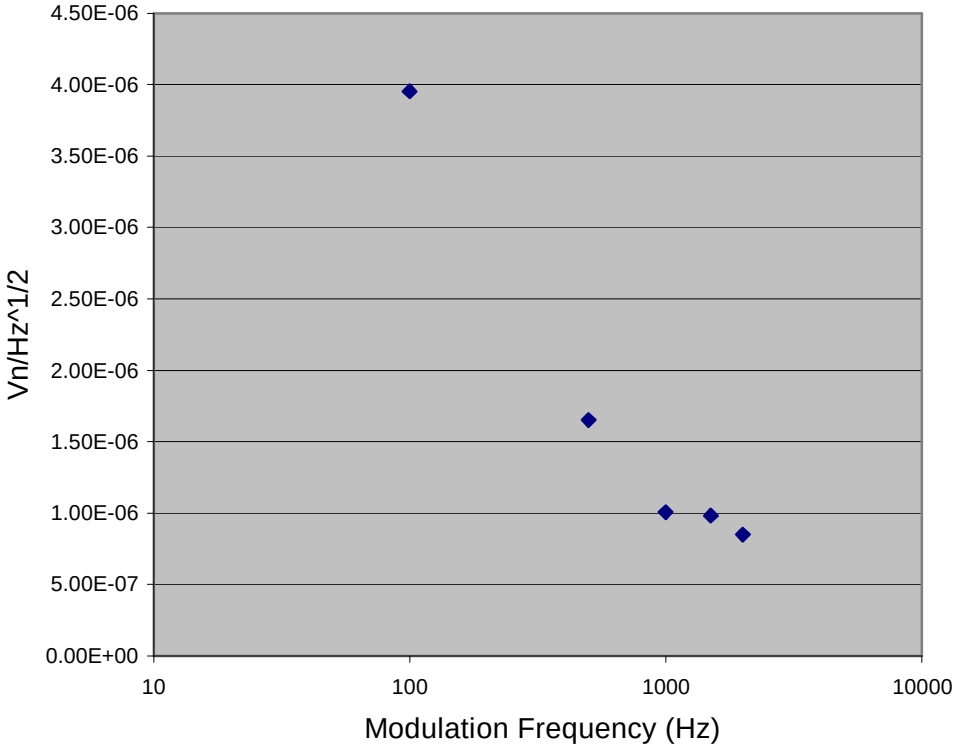

Figure 5.16 Voltage noise as a function of frequency for microbolometer. The noise was measured over a bandwidth of 10% of the selected frequency. Resonant dielectric cavity enhanced microbolometer is biased at 100 μA.

5.5 Summary

In this chapter**,** several characteristics of microbolometers were evaluated such as thermal impedance, TCR, resistance versus dissipated over power, and responsivity at room temperature and ambient pressure. The TCR of chromium as a bolometer layer is 0.0005 1/K, and the thermal impedance of the micromachined bolometer was measured to be on the order of 10^4 K/W. The experimental results

indicate that thermal impedance measured is dominated by convective cooling. Infrared measurement for the incident signal is performed in the microbolometer. For the monochromatic HeNe laser at 1.15 and 3.39 μm, the results fit within irradiation expected, 20% of calculated response. For the broadband ultrafast laser at the peak wavelengths of 2.75, 3.25, 4, and 4.5 μm, the optical response follows the trend, but results in some ambiguity. 1/f noise is dominant for this device. NEP is calculated as 5×10^{-8} W/$(Hz)^{-1/2}$ at a modulation frequency of 1500 Hz. From the result of NEP, The detectivity (*D**) at the 1500 Hz modulation frequency can be calculated as 6.9×10^{4} cm $(Hz)^{1/2}$ /W by using Eqn.2.9.